

FUNCTIONAL MAGNETIC RESONANCE IMAGING (fMRI) AND EFFECTS OF L-DOPA ON VISUAL FUNCTION IN NORMAL AND AMBLYOPIC SUBJECTS

BY Gary L. Rogers MD

ABSTRACT

Purpose: To evaluate the effects of a single dose of levodopa on visual cortex, based on functional MRI (fMRI), and on visual function, based on psychophysical tests, in amblyopic and normal subjects.

Method: A prospective, randomized trial of a single dose of levodopa (2 mg/kg body weight) was undertaken in an institutional setting in nine normal and six amblyopic subjects, who were assessed at baseline and 90 minutes after levodopa ingestion. fMRI of occipital visual cortex was undertaken with a 1.5T GE MRI scanner utilizing the BOLD contrast technique. fMRI stimuli were two gratings (0.5, 2.0 cycles/degree of visual angle) that counterphased at 4 Hz. fMRI parameters for analysis included AREA and LEVEL of activation and a SUMMED score (AREA \times LEVEL). Psychophysical tests included visual acuity, contrast sensitivity, stereoacuity, and binocular fusion.

Results: At baseline, AREA of activation ($P = .05$) and SUMMED score ($P = .05$) were significantly less in the amblyopic compared to the dominant eyes. Psychophysically, visual acuity and contrast sensitivity were significantly worse in the amblyopic eye. Following levodopa ingestion, there was significant decrease in LEVEL of activation in the amblyopic eye, even though visual acuity showed significant improvement ($P = .03$). Also, amblyopes showed a significant increase and normals showed some decrease in interocular difference in LEVEL of activation ($P = .04$).

Conclusion: Unique information was obtained when fMRI was utilized to assess visual cortical function. While levodopa improved visual acuity in the amblyopic eye, it decreased the LEVEL of activation based on fMRI, a counterintuitive finding. The results highlight the value of utilizing fMRI to assess amblyopia and provide new directions for research.

Trans Am Ophthalmol Soc 2003;101:395-410

INTRODUCTION

Amblyopia, one of the leading causes of loss of vision in children, affects approximately 2.5% of the general population.¹⁻⁵ Amblyopia is defined as reduced vision in one and sometimes two eyes during the developmental stages of the visual system, which cannot be explained by optical factors. Amblyopia is usually associated with anisometropia and/or strabismus.⁵ Most amblyopia can be corrected by a penalization method, which often involves occlusion of the dominant eye during the early stages of life.^{6,7} Although occlusion treatment is successful in the majority of cases, there is a small percentage of cases in which it is not effective.⁷⁻⁹ Further, even with successful occlusion treatment, there can be significant recidivism once occlusion is terminated for amblyopia.⁵

Occlusion therapy has been in use for more than 200 years.¹⁰ While atropine-based penalization has recently gained acceptance,¹¹ the general approach to amblyopia

therapy has remained the same—penalize the dominant eye and promote use of the amblyopic eye. A new approach to therapy, however, has recently been proposed for amblyopia; it is based on pharmacologic intervention and the use of certain precursors for neuromodulators and neurotransmitters within the brain. Gottlob and Stangler-Zuschrott¹² were the first to assess the effects of a dopamine precursor, levodopa, on visual function in adults with amblyopia. They found that levodopa improved contrast sensitivity in the amblyopic eye when compared to a placebo.¹¹ They also found that levodopa decreased the size of the suppression scotoma in the amblyopic eye compared to placebo.^{12,13}

Capitalizing on the work of Gottlob and Strangler-Zuschrott, Leguire and colleagues¹⁴ confirmed the original findings that levodopa decreased scotoma size in the amblyopic eye. Further, Leguire and colleagues¹⁴⁻¹⁸ discovered that levodopa improved visual acuity,¹⁵⁻¹⁸ visual evoked responses (VERs),¹⁶ and contrast sensitivity¹⁶ in the amblyopic eyes of older children.

As demonstrated by the studies of Gottlob and Strangler-Zuschrott^{12,13} and Leguire and colleagues,¹⁴⁻¹⁸ amblyopic deficits in humans are typically assessed with

From the Department of Ophthalmology, Ohio State University; and Children's Hospital, Columbus, Ohio. This work was supported in part by the Ohio Lions Eye Research Foundation.

psychophysical tests, including visual acuity and contrast sensitivity. Recent technological and methodological advances, however, have opened a new frontier for assessment of visual function based on functional imaging. Demer and colleagues¹⁹⁻²¹ used positron emission tomography (PET) and single-photon emission computed tomography (SPECT) to conduct functional imaging studies in human amblyopia. They found decreased function in the visual cortex of amblyopic adults as compared to normal adults. However, a major drawback to PET scanning is the need for radioactive isotopes.

Functional magnetic resonance imaging (fMRI) overcomes many of the limitations of PET scanning.²² A true benefit of fMRI over PET is the use of blood as a contrast agent and avoidance of radioactive isotopes. In addition, fMRI can be undertaken repeatedly over a short period of time (eg, minutes). fMRI has found widespread use as a tool for basic and clinical research on brain function in terms of site, level, and spatial extent of neural activation associated with a sensory or cognitive event.

Algaze and colleagues²³ were one of the first to utilize fMRI to assess differences between amblyopic and normal adults. They found that the level and extent of activation of occipital visual cortex elicited by stimulation of the amblyopic eye was less than that found with the dominant eye. The area of activation driven by monocular stimulation of the amblyopic eye was about 50% less than that of the dominant eye. Further, they found that interocular differences in the level and extent of activation were different

between amblyopes and normals. Amblyopes exhibited a significantly larger interocular difference in activation compared to normals. Algaze and colleagues²³ concluded that fMRI is sensitive to amblyopia-related deficiencies in the human occipital visual cortex and that fMRI is a potential tool for the assessment of human amblyopia.

The present study capitalizes on the use of levodopa to improve vision in amblyopic children and the use of fMRI to assess visual cortical function in amblyopic adults. The purpose of this study is to examine the effects of levodopa on visual function and on fMRI parameters, and to compare fMRI with traditional psychophysical tests in normal and amblyopic adults.

METHODS

SUBJECTS

The Human Subjects Institutional Review Board at Children's Hospital approved the study. Fully informed, signed consent was obtained from each subject, and parents where applicable, prior to the start of the study.

Normal subjects (N = 9) had no history of amblyopia and had normal visual acuity, normal contrast sensitivity, and normal stereoacuity. Amblyopic subjects (N = 6) included four with a history of anisometropia, one with a history of strabismus, and one with a history of strabismus with anisometropia. Mean visual acuity in the amblyopic subjects was 0.72 (20/105; range, 0.5-1.02) in the amblyopic eye and -0.03 (20/19) in the dominant eye. Table I

TABLE I: DEMOGRAPHIC INFORMATION OF NORMAL AND AMBLYOPIC SUBJECTS

NORMALS						
NO.	AGE (YR)	GENDER	VISUAL ACUITY		REFRACTION	
			OD	OS	OD	OS
N1	64	F	-0.2	-0.24	Plano	Plano
N2	50	M	-0.26	-0.2	-8.75 +.25 × 171	-8.00
N3	59	M	0	0	-5.0 +1.0 × 180	-5.5 + 2.50 × 180
N4	29	F	-0.28	-0.26	Plano	Plano
N5	25	F	-0.26	-0.24	Contacts	Contacts
N6	22	F	-0.28	-0.06	Contacts	Contacts
N7	29	F	-0.2	-0.22	-3.25 + .75 × 31	-3.75 +.25 × 137
N8	25	F	-0.22	-0.14	Plano	+1.50 -1.25 × 170
N9	23	F	-0.14	-0.22	-2.50 -.25 × 15	+1.50 -1.25 × 170
Mean=	36.22		-0.20	-0.18		
SD=	16.63		0.09	0.09		

AMBLYOPES			DOMINANT AMBLYOPIC		TYPE OF AMBLYOPIA		DOMINANT EYE
A1	56	M	-0.1	1.02	+5.0 +2.25 × 6	+4.25 +2.2 × 126	Anisometropic Right
A2	16	M	-0.12	0.5	+5.50 +0.25 × 77	+0.5 +0.5 × 51	A&S Left
A3	31	F	-0.1	<1.0	0.0 +2.5 × 11	Plano	Anisometropic Left
A4	47	F	-0.1	0.94	-3.0 +2.25 × 90	-.75 +3.5 × 80	Anisometropic Right
A5	16	M	-0.14	0.92	Contacts	Contacts	Anisometropic Right
A6	16	F	-0.2	0.72	-.75 +.50 × 159	-1.5 +.50 × 22	Strabismic Left
Mean=	30.33		-0.13	0.82			
SD=	17.63		0.04	0.21			

shows demographic information for the normal and amblyopic subjects.

DESIGN AND PROCEDURE

Psychophysical Vision Tests

Prior to testing, uncorrected refractive errors were determined using a Nidek autorefractor, and optical errors, if any, were corrected when necessary. Otherwise, the subject wore his or her current prescription lenses, and the same prescription was used for construction of fMRI-compatible glasses. Subjects who wore contact lenses wore their contacts throughout the test session, including during the fMRI session. Contact lens wearers also wore the MRI-compatible glasses; however, no lenses were provided.

Assessment of vision included the following psychophysical tests: visual acuity, contrast sensitivity, stereoacuity, and fusion. Visual acuity was measured with three logMAR visual acuity charts (ETDRS, Lighthouse for the Blind, New York, NY) presented in random order and with a 10-alternative forced-choice procedure as previously described.¹⁴ Contrast sensitivity functions (CSFs) were determined with three VCTS 6500 test charts (Vistech Consultants, Inc, Dayton, Ohio) presented in random order and with a 3-alternative forced-choice procedure as previously described.¹⁵ Stereoacuity was determined using the Randot stereoacuity test (Stereo Optical Co, Chicago, Ill) with a 3-alternative forced-choice procedure. Binocular fusion was determined with the red/green Worth four-dot fusion test. Fusion was measured at two viewing distances (2 feet and 10 feet). In addition, if the subject had fusion at 2 feet and suppression at 10 feet, the Worth 4-dot flash light was systematically varied between the two distances to gain an estimate of suppression scotoma size as previously described.¹⁴

Functional MRI

A back-projection system, which consisted of custom-designed and -built components and an LCD projector (Sony VPL-X1000) fitted with a custom lens (Buhl Optical, Pittsburgh, Pa), was employed to deliver visual stimuli within the bore of the MRI scanner. The stimuli were back-projected onto a screen mounted on the head coil and visible to the subject through a tilted mirror. Peripheral vision was limited with the use of MR-compatible glasses, which also served to correct refractive error. Subjects were given a hand-held occluder to facilitate monocular stimulation. The occluder prevented direct, central visual stimulation of the occluded eye.

Visual stimuli were generated on a personal computer with the aid of the Pixx software package (Concordia University Vision Laboratory, Canada). Visual stimuli were vertical sinusoidal gratings. The spatial frequencies

of the sinusoidal gratings were 0.5 and 2 cycles per degree of visual angle. Grating contrast was kept constant at 50%, where contrast was defined by the following equation:

$$\text{Contrast} = [(I_{\text{max}} - I_{\text{min}}) \times 2] / (I_{\text{max}} + I_{\text{min}}),$$

where I_{max} and I_{min} refer to maximum and minimum luminance of the grating, respectively. Stimuli were counterphased at 4 Hz, a frequency reported to enhance occipital cortex blood flow.²⁴ Each condition comprised four consecutive on-off epochs (48 seconds each). The *on* condition consisted of a particular grating and the *off* condition was darkness (Figure 1). Each stimulus was presented monocularly to each eye and binocularly in random order.

Functional MRIs were undertaken with a 1.5T GE Signa scanner at Columbus Children's Hospital. A high-resolution T2-weighted anatomical scan was first acquired for localization of the activation maps. The functional scans were acquired with a gradient-recalled echo planar (EPI) pulse sequence (TR = 3 seconds, TE = 40 milliseconds, 5-mm slice thickness, 20 to 22 cm² FOV, 64 × 64 matrix). The pulse sequence was susceptible to T2-based BOLD contrast. Eight oblique slices, parallel to the calcarine fissure, were taken in each condition for each subject.

After baseline psychophysical vision testing, each subject was placed in the MRI scanner. In the first echo-planar scan, facial and head landmarks were established to maintain anatomical areas for the first (baseline) and second (postlevodopa) scans. After the baseline scan, each subject was given an oral dose of 2.0 mg/kg body weight of levodopa, with a 25% fixed dose combination of carbidopa, a peripheral decarboxylase inhibitor (Sinemet, known as L-dopa).

Psychophysical vision testing was again performed 90 minutes following the single dose of L-dopa. The sequence of testing was the same except autorefraction was omitted. The logMAR visual acuity and CSF charts were randomized to prevent memorization and to mini-

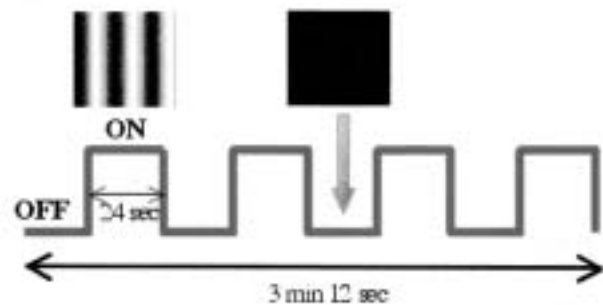


FIGURE 1

The on-off sequence of the stimulus presented to the subject.

mize learning effects. Immediately following the psychophysical tests, fMRIs were again performed.

Functional MRI Data Analysis

The fMRI data were extracted using the well-established correlation method²⁵ utilizing the Analysis of Functional NeuroImages (AFNI) software package.²⁶ A square-wave vector was used as a reference vector for calculating each voxel's time-course correlation coefficient. This reference vector was shifted by 3 seconds to accommodate for hemodynamic delay. Only those voxels surpassing a positive correlation coefficient threshold of 0.4583 ($P = .0095$) were considered as activated by the visual task. Negatively correlated voxels were excluded from further analysis. The intensity of a voxel's activation was determined as a percent change from the baseline parameter. This normalized measure of fMRI signal strength was used for within and between group comparisons. Voxel time-courses were detrended with a linear function to compensate for systematic drifts in voxel intensity that may occur over the course of the experiment.

With the aid of the high-resolution scans, delineation of the region of interest (ROI) was performed manually with a cursor. (Figure 2) Two response parameters were determined from each ROI, per stimulus condition for each subject:

LEVEL: The average of the fMRI signal percent change value per voxel, within the ROI. This parameter characterized the mean level of activation.

AREA: Equivalent to the number of voxels passing the correlation threshold. This parameter characterized the area of activation.

SUMMED: The SUMMED parameter reflects the combination (product) of the level and of the area of acti-



FIGURE 2

An fMRI scan highlighting the region of interest in the occipital cortex. Within this region, LEVEL of activation, AREA of activation, and a SUMMED (LEVEL \times AREA) were calculated.

vation in one pooled parameter.

In order to characterize differences between monocular fMRI responses, an absolute percent difference (APD) parameter was defined as follows:

$$APD = \frac{| \text{EYE1 Response} - \text{EYE2 Response} |}{\text{MAX}(\text{EYE1 Response}, \text{EYE2 Response})} * 100$$

where "Response" refers to the response parameter (LEVEL, AREA, or SUMMED) within the ROI. The absolute value of the numerator in the APD parameter yields an unsigned difference, which thus allows comparison between normal and amblyopic populations. APD, being an absolute difference measure, avoids the ambiguity in the meaning of eye dominance for normal subjects. In studying monocular stimulation, EYE1 and EYE2 were tabulated as the dominant and amblyopic eye in amblyopes and right and left eye in normal subjects.

Monocular data were subjected to a two-factor ANOVA performed on the APD parameter, using population (normal and amblyopic) and stimulus (two grating spatial frequencies) as factors. Such analysis permitted assessment of interocular area and level of activation differences between normal and amblyopic subjects as well as between stimuli.

The APD parameter is a subject-normalized ratio that allows assessment of differences between the responses in question. In order to determine which response tended to be higher, on average, the APD parameter was calculated without the absolute value, forming a signed percent difference.

Similar to the APD parameter, an absolute interocular difference (AID) parameter for binocular data was expressed as:

$$AID = \frac{| \text{BINOCULAR Response} - \text{MONOCULAR Response} |}{\text{MAX}(\text{BINOCULAR Response}, \text{MONOCULAR Response})} * 100$$

where "MONOCULAR" stands for either dominant, amblyopic, OD, or OS. To assess activation discrepancies of the binocular and monocular responses between populations, two-factor ANOVA was performed on the AID parameters using population and stimulus as factors. Two-factor ANOVA was performed separately on data from each population to assess binocular versus monocular AID differences within each population. Stimulus and difference (with two levels, ie, [OU-EYE1] AID and [OU-EYE2] AID) also served as factors.

RESULTS

VISUAL ACUITY

Figure 3 shows mean logMAR visual acuity, at baseline, for the dominant and amblyopic eyes and for OD and OS. Mean visual acuity in the dominant eye was -0.03 (20/19).

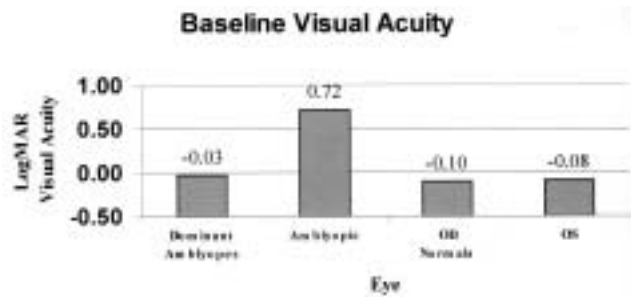


FIGURE 3

Baseline logMAR visual acuity is shown for dominant and amblyopic eyes and for OD and OS. No statistically significant differences were found among OD, OS, and dominant eyes. Visual acuity was significantly worse in amblyopic eyes.

The amblyopic eye had a mean visual acuity of 0.72 (20/105), which was significantly reduced from the dominant eye ($P = .0002$). Mean visual acuity was -0.10 (20/16) in OD and -0.08 (20/17) in OS. Mean logMAR visual acuities among OD, OS, and dominant eyes were not significantly different.

Figure 4A shows the effects of L-dopa on visual acuity in OD and OS. There was no significant change in visual acuity in OD ($P = .112$) or OS ($P = .224$) following L-dopa ingestion. Figure 4B shows the effects of L-dopa on visual acuity in the dominant and amblyopic eyes. Visual acuity did not show a significant change in the dominant eyes ($P = .23$). Visual acuity showed a significant improvement in the amblyopic eyes, from 0.72 (20/105) to 0.64 (20/87, $P = .03$), following L-dopa ingestion.

CONTRAST SENSITIVITY

Individual CSFs from the amblyopic eyes and the mean CSF of the dominant eyes are shown in Figure 5. At baseline, for each subject, the CSF of the amblyopic eye was depressed at all spatial frequencies (type II CSF loss) compared to the dominant eye. An exception was subject A2, who demonstrated a loss of contrast sensitivity only at higher spatial frequencies (type I CSF loss). This ambly-

opic subject also had the best visual acuity in the amblyopic eye (0.40, 20/50).

Figure 6 illustrates the average CSFs for OD, OS, and the dominant eyes; the CSFs are very similar. On the other hand, the mean CSF of the amblyopic eyes was significantly reduced at all spatial frequencies compared to the dominant eye ($P = .0002$).

L-dopa had no significant effect on contrast sensitivity at any spatial frequency in OD and OS. The effects of L-dopa on the CSFs from the dominant and amblyopic eyes are shown in Figure 7. Overall, no significant effect of L-dopa could be demonstrated on the CSF from the dominant or amblyopic eyes.

To further assess the effects of L-dopa on contrast sensitivity, the CSF from each subject was collapsed into a single value known as weighted mean contrast sensitivity (WMCS). WMCS equals the mean of the summed products of each spatial frequency multiplied by the corresponding contrast sensitivity. The WMCS is weighted toward the higher spatial frequencies because amblyopia usually affects the higher more than the lower spatial frequencies. Such weighting, it is believed, would make it more likely to detect significant differences. Figure 8 shows a bar graph of WMCS of the dominant and amblyopic eyes and for OD and OS. No significant differences were found between OD and OS or between the normal eyes and dominant eyes at baseline or following L-dopa ingestion. A significant difference in WMCS was found between the dominant and amblyopic eyes at baseline ($P = .0006$) and following L-dopa ingestion ($P = .003$). However, there was no significant change in WMCS following L-dopa ingestion from baseline for either the dominant ($P = .23$) or amblyopic ($P = .43$) eyes.

BINOCULAR FUNCTION

Fusion

Table II shows Worth 4-dot fusion test results at baseline (pre L-dopa) and approximately 90 minutes following L-

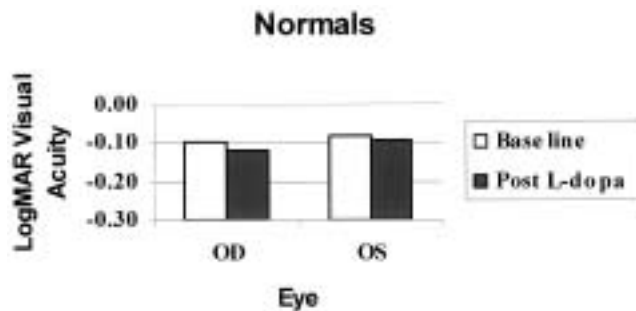


FIGURE 4A

LogMAR visual acuity is shown for OD and OS at baseline and approximately 90 minutes following L-dopa ingestion. No statistically significant differences were observed following L-dopa ingestion.

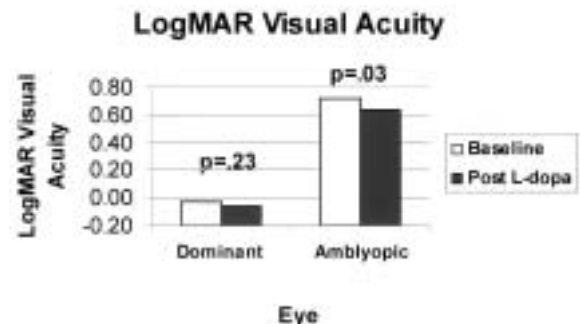


FIGURE 4B

LogMAR visual acuity is shown for dominant and amblyopic eyes. While there was no significant difference in the dominant eyes, the amblyopic eyes showed a significant ($P = .03$) decrease or improvement in visual acuity following L-dopa ingestion.

Comparison of CSFs in Amblyopic Eyes

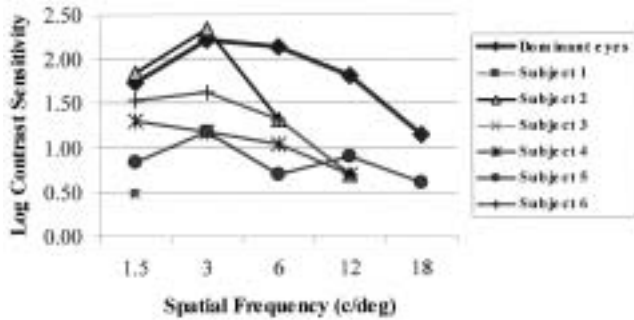


FIGURE 5

The mean contrast sensitivity function (CSF) from dominant eyes and individual CSFs from the amblyopic eyes are shown for each of the six amblyopic subjects. All amblyopic subjects showed a loss of contrast sensitivity at all spatial frequencies (type II CSF loss), except for subject A2, who showed a loss of contrast sensitivity only at the higher spatial frequencies (type I CSF loss).

CSFs in Normals and Amblyopes

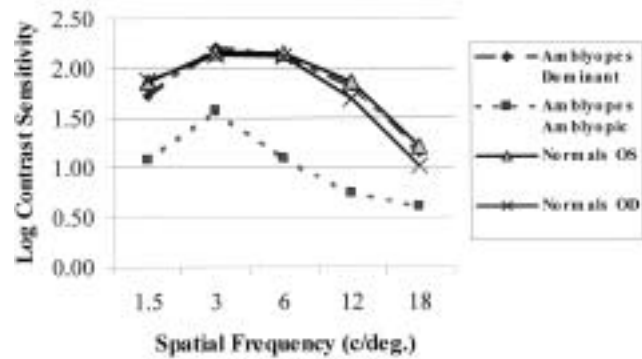


FIGURE 6

Contrast sensitivity functions are shown for dominant and amblyopic eyes and for OD and OS. The amblyopic eyes, on average, demonstrate a significant loss of contrast sensitivity at all spatial frequencies.

Effects of L-dopa on CSF

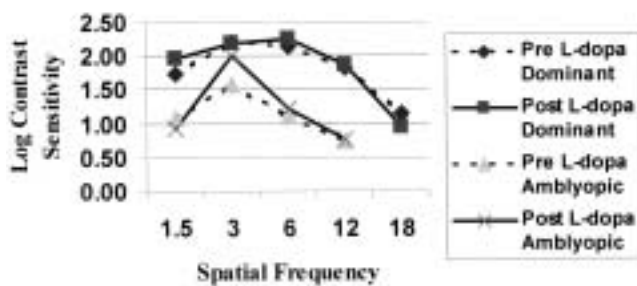


FIGURE 7

Contrast sensitivity functions are shown for dominant and amblyopic eyes before (pre L-dopa) and approximately 90 minutes following drug ingestion (post L-dopa). No significant differences were found at any spatial frequency when a comparison was made pre and post L-dopa.

dopa ingestion (post L-dopa) for amblyopic and normal subjects. Except for one subject (A2), the amblyopic subjects maintained suppression (S) at both viewing distances. Subject A2 showed about a 50% reduction in scotoma size, based on the distance at which the fusion-suppression break occurred, as listed in inches. The normal subjects demonstrated binocular fusion (Y) at both viewing distances at baseline and following L-dopa ingestion.

Stereoacuity

Table III shows the results from the Randot stereoacuity test at baseline (pre L-dopa) and approximately 90 minutes following L-dopa ingestion (post L-dopa). All amblyopic subjects maintained worse than 400 seconds of arc stereoacuity. The normal subjects varied little from baseline to the follow-up test session. In normals, stereoacuity averaged about 39 seconds of arc at baseline and 34 seconds of arc following L-dopa ingestion ($P = .22$).

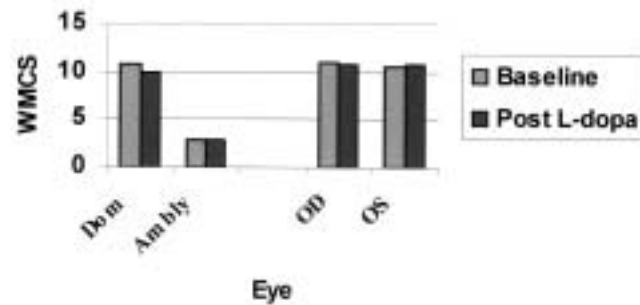


FIGURE 8

Weighted mean contrast sensitivity (WMCS) is shown for dominant (Dom) and amblyopic (Ambly) eyes and for OD and OS at baseline and approximately 90 minutes following (post) L-dopa ingestion. No significant effects of L-dopa were found on WMCS.

FUNCTIONAL MRI

Figure 9 (left) shows, for an amblyopic subject, fMRIs and the activated regions (voxels) of occipital visual cortex before (pre L-dopa) and 90 minutes following L-dopa ingestion (post L-dopa). Also shown in Figure 9 (right) are the changes over time of an fMRI voxel level of activation (thin lines) and grouped voxel activation data (course lines) for one amblyopic subject.

Figure 10 shows the mean area of activation, pre and post L-dopa, for dominant, amblyopic, and binocular stimulation. A significant decrease in the area of activation was found for the amblyopic eye ($P = .04$). The decrease in area of activation was not significant for the dominant eye ($P = .50$) or for binocular stimulation ($P = .12$), although the decreasing trend is evident in both conditions.

Figure 11 shows a significant interaction ($P = .03$) between L-dopa treatment and population (amblyopes versus normals) for the binocular AREA of activation. As

TABLE II: WORTH 4-DOT FUSION TEST RESULTS

FUSION		
AMBLYOPES	PRE L-dopa FUSION	POST L-dopa FUSION
A1	S	S
A2	32.5°	73.82°
A3	S	S
A4	S	S
A5	S	S
A6	S	S

FUSION		
NORMALS	PRE L-dopa FUSION	POST L-dopa FUSION
N1	Y	Y
N2	Y	Y
N3	Y	Y
N4	Y	Y
N5	Y	Y
N6	Y	Y
N7	Y	Y
N8	Y	Y
N9	Y	Y

S - Suppression
 Y - Fusion
 °Distance, in inches, where change occurred from suppression to fusion:

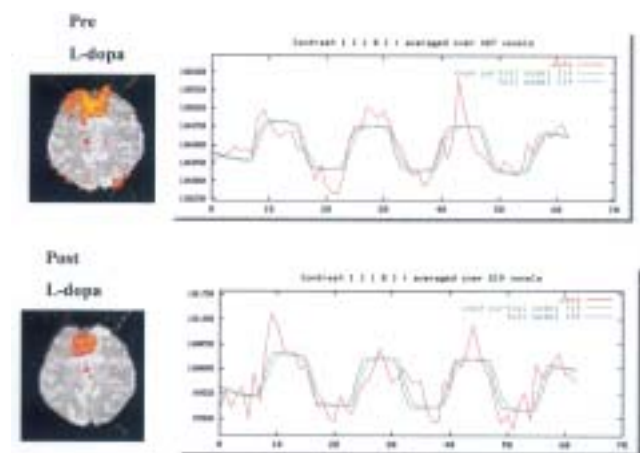


FIGURE 9

Left, fMRI images with the activated voxels (units of measurement) within the activated region of interest (ROI), in pre L-dopa and post L-dopa conditions. Right, graph illustrates time-course of activation for a group of voxels and the best-fit model of the data.

shown in Figure 11, amblyopes showed a smaller binocular AREA of activation, while normals tended to show a larger binocular area of activation following L-dopa administration. In normals, AREA of activation was not significantly different between the normal right and left eyes before and following L-dopa ingestion.

TABLE III: RESULTS FROM RANDOT STEREOACUITY TEST

STEREOACUITY		
AMBLYOPES	PRE L-dopa STEREOACUITY	POST L-dopa STEREOACUITY
A1	>400	>400
A2	>400	>400
A3	>400	>400
A4	>400	>400
A5	>400	>400
A6	>400	>400

STEREOACUITY		
NORMALS	PRE L-dopa STEREOACUITY	POST L-dopa STEREOACUITY
N1	30	20
N2	20	20
N3	70	50
N4	20	30
N5	20	20
N6	20	20
N7	50	50
N8	70	70
N9	50	30
Mean =	38.89	34.44
SD=	21.47	18.10

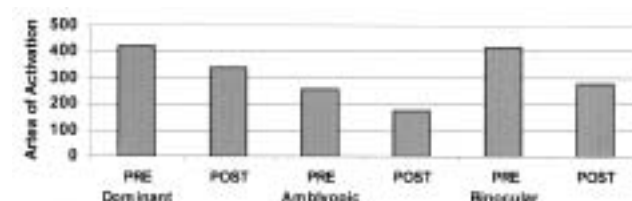


FIGURE 10

fMRI area of activation, pre and post L-dopa, is shown for dominant and amblyopic eyes and with binocular stimulation. Only the amblyopic eyes showed a significant decrease in the area of activation following L-dopa ingestion.

RELATION BETWEEN VISUAL ACUITY AND FUNCTIONAL MRI

To assess relations among logMAR visual acuity and fMRI parameters at baseline, logMAR visual acuity was correlated with the AREA of activation, LEVEL of activation (Z-score), and the SUMMED score for combined data from the normal and amblyopic subjects (n = 12). To combine data from the two groups of subjects for this analysis, the dominant eye was arbitrarily grouped with the normal right eye and the amblyopic eye was grouped with the normal left eye. To compensate for multiple comparisons, a more conservative P value of .025 was used to define a statistically significant effect.

LogMAR visual acuity in the right/dominant and left/amblyopic eyes did not significantly correlate with fMRI AREA of activation with right, left, or binocular stimulation. LogMAR visual acuity in the right/dominant

and left/amblyopic eyes also did not significantly correlate with fMRI LEVEL of activation (Z-score) or with the fMRI SUMMED score with right/dominant, left/amblyopic, or binocular stimulation.

RELATION BETWEEN CONTRAST SENSITIVITY AND FUNCTIONAL MRI

To assess relations among contrast sensitivity and fMRI parameters at baseline, WMCS was correlated with the AREA of activation, LEVEL of activation (Z-score), and the SUMMED score for the combined data from the normal and amblyopic subjects ($n = 12$). To combine data from the two groups of subjects, the dominant eye was arbitrarily grouped with the normal right eye and the amblyopic eye was grouped with the normal left eye. To compensate for multiple comparisons, a more conservative P value of .025 was used to define a statistically significant effect.

WMCS of the right/dominant eye was found to significantly correlate with fMRI area of activation at 0.5 cycles/degree grating ($P < .02$, $R = .65$, $df = 10$, Figure 12). WMCS of the left/amblyopic eye was found to significantly correlate with fMRI area of activation at the 2.0 cycles/degree grating ($P < .02$, $R = .64$, $df = 10$, Figure 13). WMCS of the right/dominant ($P < .001$, $R = 0.83$, $df = 10$, Figure 14) and of the left/amblyopic ($P < .01$, $R = 0.68$, $df = 10$, Figure 15) eyes showed statistically significant correlations with fMRI LEVEL of activation (Z-score) at 0.5 cycles/degree. WMCS of the left/amblyopic eyes also showed a statistically significant correlation with fMRI Z-score at 2.0 cycles/degree ($P < .005$, $R = 0.72$, $df = 10$, Figure 16). WMCS for the right/dominant eye showed a statistically significant correlation with the fMRI SUMMED score for the 0.5 cycles/degree grating ($P < .01$, $R = .67$, $df = 10$, Figure 17). WMCS for the left/amblyopic eye also showed a statistically significant correlation with the fMRI SUMMED score for the 2.0 cycles/degree grating ($P < .015$, $R = .64$, $df = 10$, Figure 18).

DISCUSSION

FOUNDATIONS IN ANIMAL RESEARCH

Hubel and Wiesel²⁷⁻³¹ pioneered early work on the anatomical and physiological properties of visual cortical cells and laid the foundation for our current understanding of the pathophysiology of amblyopia. Based on their animal models, it is believed that amblyopia is the result of competition between each eye's input to visual cortex during early stages of visual development. Through single cell recordings from the visual cortex of kittens and monkeys, Hubel and Wiesel discovered alternating ocular dominance columns of visual cortical cells that responded selectively to stimulation of the left or right eyes.²⁸⁻³¹ They

also found that after one eye was occluded for a period of time, the eye that remained open took control of most visual cortical cells.²⁹ That is, the majority of visual cortical cells responded to stimulation of the opened eye, and a reduced number of cells responded to stimulation of the occluded, deprived eye. Thus, amblyopia appears to reflect the consequence of competition between each eye's input to visual cortical cells, a process now known as binocular competition. Binocular competition is dependent on age, however, and the period of susceptibility encompasses the "plastic," or "critical," period of visual development.

The critical period of visual development, as defined by the development of and recovery from amblyopia, appears dependent on numerous factors besides age, including the presence of certain neurotransmitters and neuromodulators within the brain.³²⁻³⁴ For example, Kasamatsu and colleagues³² investigated the effects of dopaminergic drugs on visual cortex as it relates to the critical period of visual development. Using animal models, they showed that the amblyopic eye could recover some function, even in older animals, when the brain was flooded with a dopaminergic drug. They also demonstrated that the deleterious effects of occlusion on binocular function could be prevented, during the critical period, if a neurotoxin (6-hydroxydopamine) was used to destroy dopaminergic terminals. This work suggests that dopaminergic drugs may influence plasticity and recovery of vision in the amblyopic eye. Ultimately, these animal studies have laid the foundation for an alternative treatment of human amblyopia, utilizing neuromodulators and neurotransmitters to augment standard penalization therapy.

VISUAL ACUITY

In the present study, it was found that a single dose of a dopamine precursor, L-dopa, significantly improved visual acuity in the amblyopic eye by 0.08 logMAR units, equivalent to 4/5 of a line on a logMAR visual acuity chart. The temporary improvement of visual acuity with a single dose of L-dopa, as found in the current study, fits well with previous L-dopa studies in both adults¹³ and children.¹⁴⁻¹⁸

In several longitudinal studies, Leguire and colleagues^{14,17,18} found that L-dopa plus part-time occlusion improved visual acuity for 5 weeks followed by a leveling-off of the effect. L-dopa with part-time occlusion improved visual acuity in the amblyopic eye by approximately two lines on a logMAR chart, a 37% improvement. Importantly, it should be noted that in the studies of Leguire and colleagues, the subjects were older amblyopic children who were no longer helped by standard penalization therapy. L-dopa plus part-time occlusion appeared more effective than occlusion plus placebo.^{14,16,17}

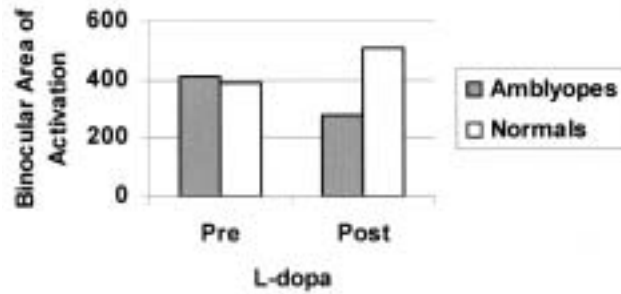


FIGURE 11

fMRI area of activation, pre and post L-dopa, with binocular stimulation is shown for normal and amblyopic subjects. The amblyopes showed a significant decrease in fMRI binocular area of activation following L-dopa ingestion.

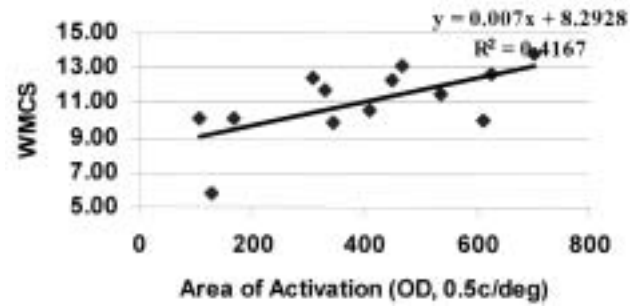


FIGURE 12

Scatter plot shows relation between weighted mean contrast sensitivity (WMCS) and fMRI area of activation at baseline for the 0.5 cycles/degree grating for the combined right eye and dominant eye data. The correlation ($R = .646$) is statistically significant ($P < .02$).

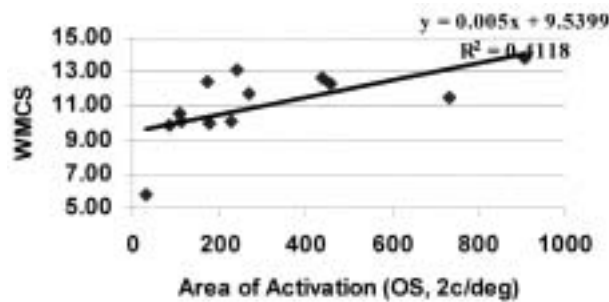


FIGURE 13

Scatter plot shows relation between weighted mean contrast sensitivity (WMCS) and fMRI area of activation at baseline for the 2.0 cycles/degree grating for the combined left eye and amblyopic eye data. The correlation ($R = .642$) is statistically significant ($P < .02$).

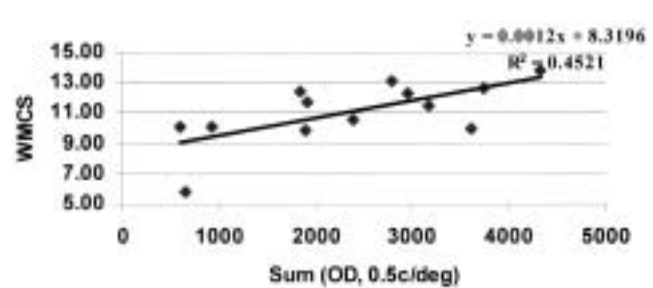


FIGURE 14

Scatter plot shows relation between weighted mean contrast sensitivity (WMCS) and fMRI level of activation (Z-score) at baseline, for the 0.5 cycles/degree grating, for the combined right eye and dominant eye data. The correlation ($R = .826$) is statistically significant ($P < .001$).

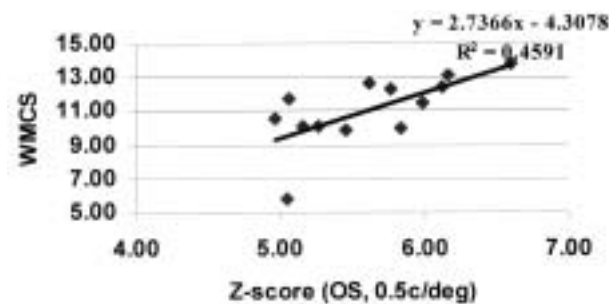


FIGURE 15

Scatter plot shows relation between weighted mean contrast sensitivity (WMCS) and fMRI level of activation (Z-score) at baseline, for the 0.5 cycles/degree grating, for the combined left eye and amblyopic eye data. The correlation ($R = .68$) is statistically significant ($P < .005$).

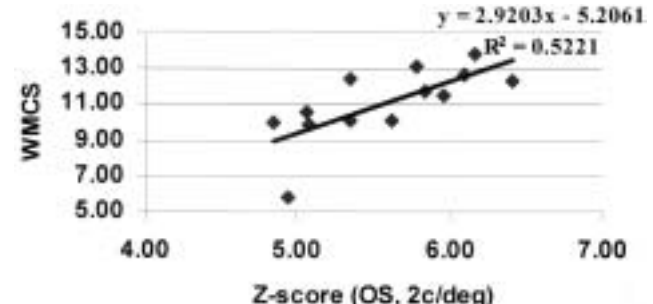


FIGURE 16

Scatter plot shows relation between weighted mean contrast sensitivity (WMCS) and fMRI level of activation (Z-score) at baseline, for the 2.0 cycles/degree grating, for the combined left eye and amblyopic eye data. The correlation ($R = .68$) is statistically significant ($P < .005$).

or placebo alone.¹⁴ Recently, these investigators showed that longitudinal dosing with L-dopa improved and reset baseline visual acuity in the amblyopic eye.³⁵ L-dopa may play an important role in the treatment of the 25% of children who do not respond to traditional penalization treatments.

L-DOPA AND TOLERANCE

In addition to uncovering the effects of L-dopa on visual function in children with amblyopia, Leguire and

colleagues¹⁴⁻¹⁸ systematically assessed side effects and tolerance of L-dopa in the pediatric population. A pharmacokinetic study was also undertaken, which revealed for the first time peak serum concentrations of L-dopa and its main metabolites (eg, dopamine, norepinephrine) in children compared to adults.¹⁵

Throughout single-dose^{15,16} and longitudinal dosing^{14,17,18} studies, Leguire and colleagues assessed blood pressure, heart rate, body temperature, and blood chemistry. Subjective side effects, such as dry mouth and

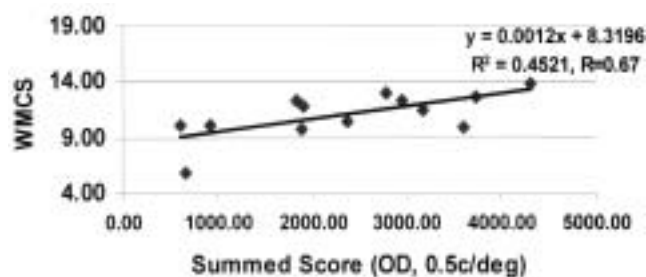


FIGURE 17

Scatter plot shows relation between weighted mean contrast sensitivity (WMCS) and fMRI SUMMED values (area \times Z-score) at baseline, for the 0.5 cycles/degree grating, for the combined right eye and dominant eye data. The correlation ($R = .67$) is statistically significant ($P < .01$).

nausea, were also assessed via questionnaire. Overall, L-dopa was well tolerated in the pediatric population. One significant finding in the study of side effects of L-dopa in the pediatric population was that longitudinal dosing of 1.02/0.25 mg/kg body weight of levodopa/carbidopa systematically decreased oral body temperature by 1.2°F over a 7-week period.³⁶ As a consequence, it has been suggested that longitudinal oral dosing with L-dopa for amblyopia should be less than 1.02 mg/kg body weight three times daily to prevent a change in body temperature.³⁶

In the present study, L-dopa was well tolerated in the normal and amblyopic adults. One amblyopic adult complained of headache, nausea, and dry mouth. One normal subject complained of headache, and another normal subject complained of dizziness. The symptoms were minor, however, and did not affect the subjects' participation in the study.

CONTRAST SENSITIVITY

It is well established that the CSF changes in children with amblyopia³⁷ as well as during penalization of the dominant eye.^{38,39} The amount of CSF loss was found to correlate with visual acuity.³⁸ When visual acuity was between 20/30 and 20/70, the loss of contrast sensitivity was restricted to the higher spatial frequencies, termed a type I CSF loss.⁴⁰ When visual acuity in the amblyopic eye was worse than 20/70, the loss of contrast sensitivity occurred at the higher and lower spatial frequencies, termed a type II CSF loss.⁴⁰ Subsequently, it was revealed that as visual acuity improved in the amblyopic eye during occlusion therapy, the CSF shifted upward, first at the lower spatial frequencies and then at the higher spatial frequencies. Thus, as visual acuity improved in the amblyopic eye through occlusion therapy, the amblyopic eye changed from a type II CSF loss to a type I CSF loss. These CSF studies in children with active and treatable amblyopia dispelled the earlier belief that type I and type

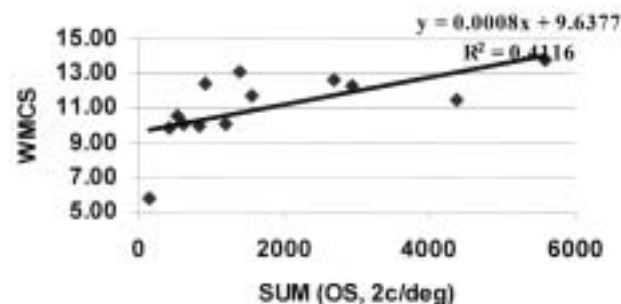


FIGURE 18

Scatter plot shows relation between weighted mean contrast sensitivity (WMCS) and fMRI SUMMED value (AREA \times Z-score) at baseline, for the 2.0 cycles/degree grating, for the combined left eye and amblyopic eye data. The correlation ($R = .64$) is statistically significant ($P < .015$).

II CSF losses reflect distinct clinical entities.⁴⁰

An important finding in those earlier studies also answered the question as to why amblyopic patients favored the dominant eye even when the (previous) amblyopic eye had the same visual acuity. The findings revealed that even though the patient obtained 20/20 Snellen acuity in the amblyopic eye and thus the amblyopia was "cured," the patient maintained a loss of contrast sensitivity.⁴¹ Apparently, visual acuity does not fully capture the quality of vision in the amblyopic eye, and contrast sensitivity may be a better index of the quality of vision. Thus, amblyopes may prefer the dominant eye because contrast sensitivity is better in the dominant eye, even though visual acuity is the same in both eyes.

A continued drawback in the use of contrast sensitivity to assess amblyopia, however, is that the contrast sensitivity function is not friendly to use in a clinical environment, is not easy to interpret, and is difficult to use to follow patients longitudinally.

WEIGHTED MEAN CONTRAST SENSITIVITY

We developed a measure referred to as weighted mean contrast sensitivity to aid in the clinical use of the CSF. The WMCS is defined by multiplying contrast sensitivity with each respective spatial frequency and taking the mean of the summed products. WMCS produces a single number to express the CSF, which makes it easier to utilize in a clinical setting. For example, WMCS makes it easier to compare interocular differences. WMCS weights or gives more emphasis to the higher spatial frequencies, where amblyopes are more likely to exhibit a loss. It also aids when there are missing data; for example, when data are missing at the higher spatial frequencies, which is typical in amblyopic eyes. WMCS also yields a value regardless of the amount of missing data, as long as at least one spatial frequency is detectable.

THE MISSING DATA QUANDRY

Table IV and the corresponding data in Figure 19 highlight a fundamental problem in the use of the CSF in both research and in clinical practice. As previously noted, amblyopes tend to exhibit losses of contrast sensitivity at the higher spatial frequencies and, as a consequence, contrast sensitivity data may not be available at all spatial frequencies for all patients or subjects. The fundamental problem is what to do with such missing data.

Table IV shows mean log contrast sensitivity at the five spatial frequencies used in the current study for the dominant (Dom) and amblyopic (Ambly) eyes. The “0” conditions signify when the subject could not detect the grating at the highest contrast level, and the data point was filled with a 0 (zero). The “empty” conditions signify when the subject could not detect the grating of a certain spatial frequency at the highest contrast level, and the individual data point for the subject was left blank. This condition is equivalent to not running the subject. In addition, an empty or blank data point would decrease the degrees of freedom and make it more likely not to find statistically significant differences in the data. In the Ambly (mean) condition, the subject’s missing data point was filled in with the mean contrast sensitivity for that spatial frequency.

Note in Table IV that the Ambly (mean) condition and the Ambly (empty) condition yield the same outcome. However, in the Ambly (mean) condition, degrees of free-

dom in the statistical tests would not be decreased as they would be in the Ambly (empty) condition, thus making it more likely to find statistical differences. The two dominant (Dom) conditions shown in Table IV are identical because there were no missing data. The amblyopic conditions shown in Table IV and the corresponding CSFs as shown in Figure 19 are different and are dependent on how the missing data were handled. Further, while Ambly (empty) and Ambly (mean) appear to provide the same CSF results, the difference in these two conditions is in the degree of freedom, which may be important in determining whether the results are statistically significant.

Replacing missing data with a zero (eg, Ambly [0]) is not appropriate for several reasons. Since contrast sensitivity is a ratio (1/contrast threshold), a contrast sensitivity of zero would be undefined. Second, it is most likely that the subject’s contrast sensitivity was above zero but worse than the highest contrast level on the CSF test for that given spatial frequency. Thus, replacing missing data with a zero is not the best choice and could lead to a greater loss of (mean) contrast sensitivity than what probably exists.

Replacing missing data with the mean contrast sensitivity for that given spatial frequency is one “solution” considered in standard statistical packages such as SPSS (Statistical Package for the Social Sciences). However, replacing missing data with the mean contrast sensitivity

TABLE IV: MEAN LOG CONTRAST SENSITIVITY AT FIVE SPATIAL FREQUENCIES

CONDITION	SPATIAL FREQUENCY				
	1.5	3	6	12	18
Dom (“0”)	1.73	2.22	2.14	1.82	1.15
Dom (empty)	1.73	2.22	2.14	1.82	1.15
Ambly (“0”)	1.08	1.05	0.73	0.50	0.10
Ambly (empty)	1.08	1.58	1.10	0.75	0.60
Ambly (mean)	1.08	1.58	1.10	0.75	0.60

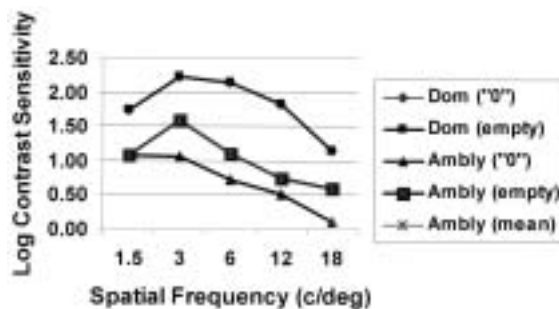


FIGURE 19

Contrast sensitivity functions (CSFs) shown in this figure correspond to data as shown in Table IV. Depending on how missing data is handled, appreciable differences are noted in the CSFs, particularly at the higher spatial frequencies and in the amblyopic eye.

for that given spatial frequency (eg, Ambly [mean]) would yield too generous a contrast sensitivity value and would tend to underestimate the true amblyopic deficit as shown in Figure 19. Yet, such a strategy would preserve the degrees of freedom for statistical analysis and make it more likely to find significant differences.

Leaving the data point empty (Ambly [empty]) would seem the best option in terms of representing the actual data; however, the average value as plotted, for example, would lead one to believe that it is a mean of all the subjects, instead of a few. Use of the Ambly (empty) option might be strengthened if the number of subjects were listed next to each data point (ie, spatial frequency) on the CSF. Unfortunately, the Ambly (empty) option

reduces the degrees of freedom for the given spatial frequency and would make it more likely not to find significant differences. In addition, when the data point is left empty, it would effectively prevent the use of some of the remaining data for analysis; for example, when whole CSF data is used for assessing population effects. Subjects missing data, even from one spatial frequency, would be dropped from such an analysis, even though most of the data were present.

The problems with utilizing the whole CSF in research and in clinical practice led us to an alternative approach, the use of WMCS as previously noted. Further, as noted in the following paragraphs, WMCS proves valuable in better understanding the relation between visual function based on WMCS and cortical visual function, based on cerebral blood flow, as demonstrated by fMRI.

RELATIONSHIP BETWEEN FUNCTIONAL MRI AND PSYCHOPHYSICAL VISION TESTS

The present study revealed only small correlations between fMRI parameters and visual acuity, which did not reach statistical significance at the 0.05 level. These findings suggest only a minor relationship between visual acuity, as measured psychophysically, and fMRI, based on cerebral blood flow. Other studies have also demonstrated minor relationships between visual acuity and fMRI.⁴² Although several studies have now shown a reduction in certain fMRI parameters in human amblyopia,^{23,42-44} it is apparent that the loss of visual acuity does not fully or even partially explain such fMRI deficits.

Perhaps it is not surprising that there is such a small relationship between visual acuity and fMRI. After all, visual acuity only reflects a subset of visual cortical cells that are tuned toward very high spatial frequencies and very small stimuli. In a sense, visual acuity is a single point along the continuum of visual function, and a single point would not relate well to a fMRI, for example, that reflects the volume of occipital visual cortex. fMRI, on the other hand, reflects blood flow to a large portion of occipital visual cortex, which would encompass visual cortical cells that are tuned to a much larger range of spatial frequencies, including those responsible for visual acuity. The relationship between visual acuity and fMRI, or the lack thereof, is clarified in Figure 20.

There is considerable evidence that the CSF is composed of a number of overlapping and independent spatial frequency channels, with each channel tuned to a restricted set of spatial frequencies.⁴⁵⁻⁴⁷ The channel on the far right of the CSF shown in Figure 20, which is tuned toward the highest spatial frequencies, would be responsible for visual acuity. In this model of vision, visual acuity reflects only a small portion of overall visual function, and thus it is not surprising that visual acuity would correlate

poorly with fMRI. At the same time, however, if the model of vision as depicted in Figure 20 is valid, a prediction would be that fMRI would correlate with CSF, as found in the present study.

As shown in Figures 12 through 18, when the CSF was collapsed into a single value defined as weighted mean contrast sensitivity, WMCS showed strong relationship with fMRI. These latter data indicate a strong relationship between the CSF and fMRI and support the prediction as outlined previously. If the channel theory of vision and of the CSF is valid, then it follows that CSF data, as reflected by the WMCS, would exhibit a higher correlation than visual acuity with fMRI. While visual acuity may reflect only one spatial frequency channel and only a restricted set of visual cortical cells, the CSF would reflect a large number of spatial frequency channels and a large set of corresponding visual cortical cells. In fact, the CSF is actually a volume-type index of vision given that vision as defined by the CSF (and WMCS) represents the area under the CSF curve. As a consequence, given that fMRI reflects cerebral blood flow to a large area of occipital visual cortex and the CSF is a type of volume index, the CSF would more fully capture the actual function of this occipital visual cortex as found in the present study.

FUNCTIONAL MRI

fMRI detected a select response to L-dopa from each population. It appeared that the changes in AREA of activation caused by L-dopa, as detected by BOLD fMRI, were limited to the amblyopic eye. In the interpretation of

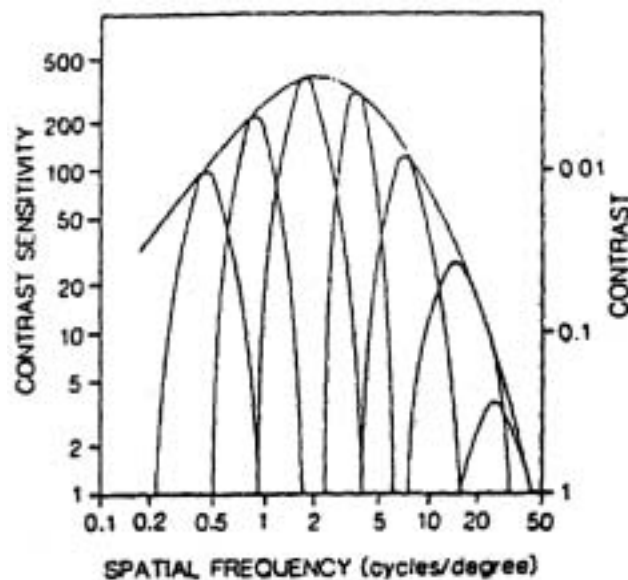


FIGURE 20

Contrast sensitivity function (CSF) is shown with corresponding spatial frequency channels. The overlapping and independent spatial frequency channels sum together to form the CSF and together reflect a wide range of cortical visual function (Reprinted with permission from Ginsburg)⁴⁶.

BOLD fMRI change as a result of L-dopa, it is important to realize the changes that take place in deoxyhemoglobin concentration as outlined by the flow chart in Figure 21.

As a consequence of the improvement in visual acuity

increased deoxyhemoglobin, and enhanced the OFF effect. This explanation is unlikely, since an L-dopa-induced increase in blood flow would be global in nature and affect both the arterial and venous sides.

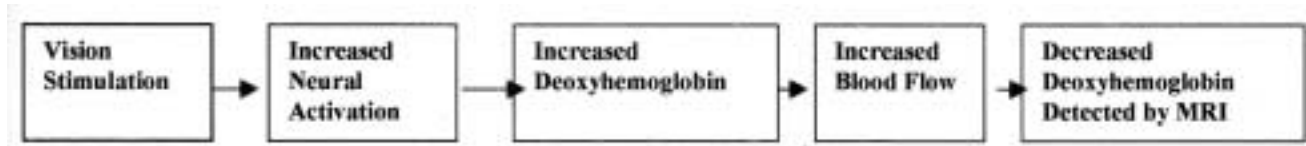


FIGURE 21

Flow diagram starting with vision stimulation and ending with decreased deoxyhemoglobin detected by fMRI.

in the amblyopic group following L-dopa, we expected to find an increase in fMRI parameters such as area of activation and more toward normal values. The counterintuitive decrease in fMRI area of activation with L-dopa from the amblyopic eye raises the possibility of several potential underlying mechanisms.

One explanation of these counterintuitive findings is based on increased metabolism caused by L-dopa. If there was increased metabolism due to L-dopa during the “on state,” more oxygen would be utilized by the activated region, and this would increase deoxyhemoglobin concentration and, consequently, reduce the on state fMRI response. As shown in Figure 1, it is possible that L-dopa caused the on-phase to decrease or/and the off-phase to increase, which would effectively reduce fMRI area of activation. However, such an explanation would seem to apply to both the dominant and the amblyopic eyes in amblyopes as well as to the left and right eyes of normals, which was not the case.

Another explanation of these counterintuitive findings is that L-dopa increased washout on the venous side,

Another explanation is based on a relative change of the relation between localized cerebral blood flow and localized cerebral oxygen metabolism.⁴⁸ With visual stimulation, neuronal activity at the synaptic level consumes oxygen and results in deoxygenated hemoglobin. At the same time, because of the increased demands for oxygen by the locally activated visual cortex, blood flow is increased to this area and the oxygen-delivered blood flow is significantly greater than the oxygen demands of the visual neurons. Thus, in adults, localized cerebral blood flow (LCBF) is greater than the localized cerebral oxygen (O₂) metabolism (LCO₂M). The oxygenated hemoglobin/deoxyhemoglobin ratio becomes greater than the resting level, and the BOLD signal is positive.

The balance between localized cerebral blood flow and localized cerebral oxygen metabolism (and fMRI response) is particularly relevant when it comes to children. In children, localized cerebral blood flow may be less than metabolic demands. Because of the immaturity of the blood flow network or the high neuronal concentrations associated with the critical period of vision development, visual stimulation may generate a negative fMRI signal in infants and young children. Mechanisms that could lead to such an effect include an immature blood flow system, high neuronal concentration as with the critical period of visual development, or alteration in the relation between inhibitory and excitatory neurons at the synaptic level. Visual stimulation could cause the oxygen demands of the localized visual cortex to exceed the oxygen increase as a result of increased blood flow. The oxygenated hemoglobin/deoxyhemoglobin ratio could be reduced or even fall below the resting level, and the BOLD signal would become negative. The fact that the BOLD fMRI signal can be reduced or even negative in young children⁴⁹ may have significance in understanding neural plasticity, drug effects on visual function, and possibly therapeutic intervention.

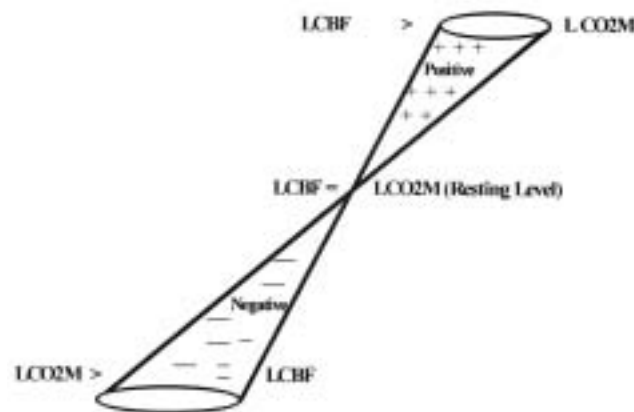


FIGURE 22

Relation between localized cerebral blood flow (LCBF), localized cerebral oxygen (O₂) metabolism (LCO₂M), and BOLD contrast signal. (Adapted with permission from *Pediatr Res.*)⁴⁹ A volume dimension has been added to the figure to simulate the relation between voxel magnitude (distance from the apex) and volume of the activated area ($R = 0.79$, $df = 10$, $P = .001$).

THE PARADOXICAL fMRI AND L-dopa EFFECT

It is known that dopamine is decreased in visual cortex as a result of deprivational amblyopia.⁴⁴ Dopamine is a

known inhibitory neurotransmitter, which produces a profound effect at the synaptic level.⁵⁰ Action potentials cause the release of dopamine into the synapse and influence dopamine receptors on postsynaptic neurons. fMRI is believed to reflect mainly synaptic activity rather than neuronal spike activity.⁵¹ As a consequence, it is possible that in amblyopia, there is a decreased availability of dopamine in visual cortex and less inhibition and more noise. Exogenous dopamine via L-dopa could increase amounts of dopamine at the synapse and increase inhibition, leading to improved signal-to-noise ratio and improved visual acuity. Modeling of the fMRI response in relation to inhibition and excitation has shown that inhibition can lower fMRI activation levels if actively driven excitation is present.⁵² These paradoxical findings warrant further research.

REFERENCES

- National Society to Prevent Blindness. *Vision Problems in the U.S. Data Analysis. Definitions, Data Sources, Detailed Data Tables, Analysis, Interpretations*. New York: National Society to Prevent Blindness; 1980. Publication P-10.
- Oliver M, Nawratzki I. Screening of pre-school children for ocular anomalies. II. Amblyopia. Prevalence and therapeutic results at different ages. *Br J Ophthalmol* 1971;55:467-471.
- Sorsby A, Sheridan M, Leary GA. Vision, visual acuity, and ocular refraction in young men. *BMJ* 1960;1394-1398.
- Hillis A, Flynn JT, Hawkins BS. The evolving concept of amblyopia: a challenge to epidemiologists. *Am J Epidemiol* 1983;118:192-205.
- Flom MC, Neumaier RW. Prevalence of amblyopia. *Public Health Rep* 1966;8:329-341.
- Mazow ML, Chuang A, Vital MC, et al. 1999 Costenbader Lecture. Outcome study in amblyopia: treatment and practice pattern variations. *J AAPOS* 2000;4:109.
- Simons K, Gotzler KC, Vitale S. Penalization versus part-time occlusion and binocular outcome in treatment of strabismic amblyopia. *Ophthalmology* 1997;104:2156-2160.
- Scott WE, Dickey CF. Stability of visual acuity in amblyopic patients after visualmaturity. *Graefes Arch Clin Exp Ophthalmol* 1988;226:154-157.
- Harrad R. The efficacy of occlusion for strabismic amblyopia. Can an optimal duration be identified? *Br J Ophthalmol* 2000;84:561.
- Buffon C. Differences in the visual performance of the two eyes. In: Noorden GN, ed. *The History of Strabismology*. Chap 1. Strabismology from its beginnings to the middle of the 19th century. IV.Theories of the etiology and pathogenesis of strabismus. Remky H, ed. Belgium: J.P. Wayenborgh; 2002:15.
- The Pediatric Eye Disease Investigator Group. A randomized trial of atropine vs patching for treatment of moderate amblyopia in children. *Arch Ophthalmol* 2002;120:268-278.
- Gottlob I, Stangler-Zuschrott E. Effect of levodopa on contrast sensitivity and scotomas in human amblyopia. *Invest Ophthalmol Vis Sci* 1990;31:776-780.
- Gottlob I, Charlier J, Reinecke RD. Visual acuities and scotomas after one-week levodopa administration in human amblyopia. *Invest Ophthalmol Vis Sci* 1992;33:2722-2728.
- Leguire LE, Rogers GL, Walson PD, et al. Occlusion and levodopa-carbidopa treatment for childhood amblyopia. *J AAPOS* 1998;2:257-264.
- Leguire LE, Rogers GL, Bremer DL, et al. Levodopa and childhood amblyopia. *J Pediatr Ophthalmol Strabismus* 1992;29:290-298.
- Leguire LE, Rogers GL, Bremer DL, et al. Levodopa/carbidopa for childhood amblyopia. *Invest Ophthalmol Vis Sci* 1993;34:3090-3095.
- Leguire LE, Walson PD, Rogers GL, et al. Longitudinal study of levodopa/carbidopa for childhood amblyopia. *J Pediatr Ophthalmol Strabismus* 1993;30:354-360.
- Leguire LE, Walson PD, Rogers GL, et al. Levodopa/carbidopa treatment for amblyopia in older children. *J Pediatr Ophthalmol Strabismus* 1995;32:143-151.
- Demer JL, von Noorden GK, Volkow ND, et al. Imaging of cerebral blood flow and metabolism in amblyopia by positron emission tomography. *Am J Ophthalmol* 1988;105:337-347.
- Demer JL, von Noorden GK, Volkow ND, et al. Brain activity in amblyopia. *Am Orthopt J* 1991;41:56-66.
- Demer JL. Positron emission tomographic studies of cortical function in human amblyopia. *Neurosci Biobehav Rev* 1993;17:469-476.
- Ochi H. Brain, heart and tumor imaging: updated PET and MRI. In: *Proceedings of the 2nd International Osaka City University Symposium on Brain, Heart and Tumor Imaging*. Osaka, Japan, Oct 2-4, 1994.
- Algaze A, Roberts CJ, Leguire LE, et al. Functional magnetic resonance imaging as a tool for investigating amblyopia in the human visual cortex. *J AAPOS* 2002;6:300-308.
- Fox PT, Raichle ME. Focal physiological uncoupling of cerebral blood flow and oxidative metabolism during somatosensory stimulation in human subjects. *Proc Natl Acad Sci USA* 1986;83:1140-1144.
- Bandettini PA, Jesmanowicz A, Wong E, et al. Processing strategies for time-course data sets in functional MRI of the human brain. *Magn Reson Med* 1993;30:161-173.
- Cox RW, Hyde JS. Software tools for analysis and visualization of fMRI data. *NMR Biomed* 1997;10:171-178.
- Wiesel TN, Hubel DH. Single cell responses in striate cortex if kittens deprived of vision in one eye. *J Neurophysiol* 1963;26:1003-1017.
- Hubel DH, Wiesel TN. Functional architecture of macaque monkey visual cortex. *Proc R Soc Lond B Biol Sci* 1977;28:198:1-59.
- Hubel DH, Wiesel TN, LeVay S. Plasticity of ocular dominance columns in monkey striate cortex. *Philos Trans R Soc Lond B Biol Sci* 1977;278:377-409.
- LeVay S, Wiesel TN, Hubel DH. The development of ocular dominance columns in normal and visually deprived monkeys. *J Comp Neurol* 1980;19:1-51.
- TN. Postnatal development of the visual cortex and the influence of environment. *Nature* 1982;299:583-591.
- Kasamatsu T, Pettigrew JD, Ary M. Restoration of visual cortical plasticity by local microperfusion of norepinephrine. *J Comp Neurol* 1979;185:163-181.

33. Kasamatsu T, Pettigrew JD. Preservation of binocularity after monocular deprivation in the striate cortex of kittens treated with 6-hydroxydopamine. *J Comp Neurol* 1979;185:139-161.
34. Imamura K, Kasamatsu T. Interaction of noradrenergic and cholinergic systems in regulation of ocular dominance plasticity. *Neurosci Res* 1989;6:519-536.
35. Leguire LE, Komaromy KL, Nairus TM, et al. Long-term follow-up of L-dopa treatment in children with amblyopia. *J Pediatr Ophthalmol Strabismus* 2002;39:326-330.
36. Leguire LE, Nairus T, Walson P. Influence of levodopa/carbidopa on body temperature in children. *Curr Ther Res* 1995;56:333-340.
37. Leguire LE, Rogers GL, Bremer DL, et al. A comparison of contrast sensitivity between strabismic and anisometropic amblyopia in children. *Binocul Vis Strabismus Q* 1989;4:179-186.
38. Leguire LE, Rogers GL, Bremer DL. Functional amblyopia is a single continuum of visual impairment on contrast sensitivity functions. *Binocul Vis Strabismus Q* 1987;2:199-208.
39. Wali N, Leguire LE, Rogers GL, et al. CSF interocular interactions in childhood amblyopia. *Optom Vis Sci* 1991;68:81-87.
40. Hess RG, Howell ER. The threshold contrast sensitivity function in strabismic amblyopia. *Vis Res* 1977;17:1049-1056.
41. Rogers GL, Bremer DL, Leguire LE. The contrast sensitivity function and childhood amblyopia. *Am J Ophthalmol* 1987;104:64-68.
42. Martin E, Joeri P, Loenneker T, et al. Visual processing in infants and children studied using functional MRI. *Pediatr Res* 1999;46:135-140.
43. Altman NR, Bernel B. Brain activation in sedated children: auditory and visual functional MRI imaging. *Radiology* 2001;221:56-63.
44. Qu Y, Eysel UT, Vandesande F, et al. Effect of partial sensory deprivation on monoaminergic neuromodulators in striate cortex of adult cat. *Neuroscience* 2000;101: 863-868.
45. Goodyear BG, Nicolle DA, Humphrey GK, et al. BOLD fMRI response of early visual areas to perceived contrast in human amblyopia. *J Neurophysiol* 2000;84:1907-1913.
46. Ginsburg AP. Spatial filtering and visual form perception. In: Boff KR, Kaufman L, Thomas JP, eds. *Handbook of Perception and Human Performance*. New York: Wiley; 1986;2(34):1-41
47. Campbell FW, Robson JG. Application of Fourier analysis to the visibility of gratings. *J Physiol* 1968;197:551-566.
48. Tollhurst DJ. Separate channels for the analysis of the shape and the movement of moving visual stimulus. *J Physiol* 1973;231:385-402.
49. Martin E, Joeri P, Loenneker T, et al. Visual processing in infants and children studied using functional MRI. *Pediatr Res* 1999;46:135-140.
50. Zhao Y, Kerscher N, Eysel U, et al. Changes of contrast gain in cat dorsal lateral geniculate nucleus by dopamine receptor agonists. *Neuroreport* 2001;17;12(13):2939-2945.
51. Medoff DR, Tagamets MA. Neural networks: neural systems III. *Am J Psychiatry* 2000;157:1571.
52. Tagamets MA, Horwitz B. Interpreting PET and fMRI measures of functional neural activity: the effects of synaptic inhibition on cortical activation in human imaging studies. *Brain Res Bull* 2001;54:267-273.